

Thermal Conductivity of a Thermosetting Advanced Composite During Its Cure

Jeffrey D. Farmer* and Eugene E. Covert†

Massachusetts Institute of Technology, Cambridge, Massachusetts 02139

The thermal conductivity of a thermosetting advanced composite material during its cure was experimentally investigated and compared to analytical models. The thermal conductivity of graphite/epoxy was experimentally measured using a guarded hot plate apparatus. The through-thickness transverse thermal conductivity of composite laminates was measured at various resin degrees of cure and fiber volume fractions while using various ply lay-up angles. The in-plane thermal conductivity was measured using unidirectional laminates, as well as laminates with various ply lay-up angles. Techniques for manufacturing composite laminates with these various properties, as well as the guarded hot plate apparatus necessary for accurate measurements, are described. Finally, various analytical models were researched, and those that compare most favorably with the experimental data are presented.

Nomenclature

H_c	= thermal contact conductance of the experiment, $W/m^2\text{°C}$
H_r	= resin heat of reaction for AS4/3501-6, J/g
K	= thermal conductivity, $W/m\text{°C}$
L	= laminate dimension in the x direction, m
N	= number of plies in a laminate
p	= function of the fiber volume fraction, Eq. (6)
Q	= total heat flux, W
q	= heat flux/area, W/m^2
\dot{q}	= resin energy generation rate per unit volume, W/m^3
q_{in}	= heat flux/area applied by the guarded hot plate, W/m^2
T	= temperature, $^{\circ}\text{C}$
t	= laminate dimension in the z direction, m
V	= volume fraction of a constituent material
W	= laminate dimension in the y direction, m
x, y, z	= laminate coordinates defined in Fig. 1
α	= resin degree of cure, scale of 0–1.0
γ	= function of material conductivities, Eq. (11)
δ	= resin rectangle side parallel to measured K , μm
ε	= resin rectangle side \perp to measured K , μm
θ	= direction of ply alignment, Fig. 1, deg
ν'	= function of material conductivities, Eq. (5)
ρ	= density, g/m^3

Subscripts

act	= actual material property
c	= experimental setup contact region property
comp	= composite property

eff	= effective material property
f	= fiber property
meas	= experimentally measured property
r	= resin property
x	= property in the x direction
y	= property in the y direction
11	= effective laminate longitudinal principal property
33	= effective laminate through-thickness transverse principal property

Introduction

THE manufacture of advanced composite materials is a very complex process that at times may result in parts of unsatisfactory quality. In recent years extensive work has been completed towards modeling the heat transfer, resin flow,^{1–3} and compaction^{4,5} of thermosetting composites during their cure. The purpose of these studies has been to model the process and, therefore, gain insight into or even optimize the cure of thermosetting composites. However, assumptions made in these models preclude their use beyond unidirectional composite laminates with constant material properties. Ghasemi Nejhad et al.⁶ did model the thermal conductivity of a three-dimensional cylindrical geometry with a helical fiber path, but this work applies to thermoplastic matrix composites.

The purpose of this work is to extend the heat transfer sections of the thermosetting composite models into the realm of multidirectional lay-ups with material properties that may change during the cure process. This work is the beginning of a fully three-dimensional process model that will have the ability to model the heat transfer in realistic parts made of thermosetting composites. The goal for this model is to enable the accurate calculation of the temperature and degree of cure profiles in a laminate during its cure, which is necessary for the prediction of residual stress and the resultant laminate warpage. Predicting the occurrence of this defect will help determine if a chosen cure cycle is appropriate for a high-quality composite laminate.

The heat transfer within thermosetting composites is governed by an energy balance that may include conductive and convective terms. It has been shown,⁵ however, that in most cases the convective term may be neglected in modeling the heat transfer during a composite's cure. Thus, this article concentrates on measuring the thermal conductivity of the graphite/epoxy (Hercules AS4/3501-6) as a function of temperature,

Presented as Paper 95-1475 at the AIAA/ASME/ASCE/AHS/ASC 36th Structures, Structural Dynamics, and Materials Conference, New Orleans, LA, April 10–12, 1995; received May 16, 1995; revision received Jan. 25, 1996; accepted for publication Jan. 27, 1995. Copyright © 1996 by the American Institute of Aeronautics and Astronautics, Inc. All rights reserved.

*Graduate Student, Department of Aeronautics and Astronautics; currently at U.S. Air Force Advanced Composites Program Office, WL/MLS-OL 5225 Bailey Loop, McClellan AFB, CA 95652-2510. Member AIAA.

†T. Wilson Professor of Aeronautics, Department of Aeronautics and Astronautics. Fellow AIAA.

resin degree of cure, fiber volume fraction, and ply lay-up angle.

Manufacturing Procedure and Experimental Setup

Manufacturing Procedure

Composite laminates with various material properties and amounts of constituent materials were required for this research. Detailed manufacturing methods and cure cycles can be found elsewhere,⁷ but a brief description of each is given in this article. The void content of the laminates was measured to be less than 1%, and so void content was not included in the measurements and calculations of this work.

The advanced composite laminates were layed up by hand using AS4/3501-6 prepreg tape, which had previously been stored in a sealed container below 0°C. The AS4/3501-6 prepreg was chosen because it is a common thermosetting composite material used by the aerospace industry and is readily available from its supplier, Hercules Inc. The prepreg was obtained from Hercules as a standard lot of material containing fibers whose typical diameter was 7–8 μm . The prepreg was cured in a Baron–Blakeslee autoclave. The test laminates were cut to their desired dimensions using a water-cooled diamond-grit cutting wheel.

Through-thickness transverse laminate thermal conductivity measurements were taken in the z direction (Fig. 1a), using laminates with $L = 12.7 \pm 0.25$ cm, $W = 12.7 \pm 0.25$ cm, and $t = 5.1 \pm 0.25$ mm. The laminates used for these measurements will be referred to as the through-thickness transverse (T^3) laminates; the T^3 laminate coordinate system is defined in Fig. 1a. Cure cycles of various lengths were designed for the manufacture of T^3 laminates with various resin degrees of cure. A cure cycle that attained a temperature of 143°C for 5 min was used to achieve a partial resin degree of cure ($\alpha = 0.5$); a cure cycle of 10 h at 177°C was used to achieve a complete resin

degree of cure ($\alpha = 0.98$). Lower laminate fiber volume fractions were achieved by using prepreg with a high resin weight fraction (50% or more) and a net resin cure. Medium laminate fiber volume fractions were achieved by using the standard AS4/3501-6 cure cycle for typical prepreg (36–42% resin weight fraction), whereas higher fiber volume fractions were achieved using the same prepreg and a cure cycle with a longer dwell time, and higher pressure, at the resin flow stage.

In-plane laminate thermal conductivity measurements (fibers aligned along the direction of conductivity measurement or at a specified angle θ to it) were taken in the x direction (Fig. 1b), using laminates with $t = 2.54 \pm 0.25$ cm, $W = 12.7 \pm 0.25$ cm, and $L = 5.1 \pm 0.25$ mm. The laminates used for these measurements will be referred to as the in-plane (IP) laminates; the IP coordinate system is defined in Fig. 1b. The IP laminates were first manufactured in a standard manner as a flat 12.7-cm-long by 3.8-cm-wide laminate with the ply longitudinal direction placed in the laminate width direction. The laminates were cut into 5.1 by 12.7 cm strips. The strips were rotated 90 deg about their long axis, and rebonded together using 3501-6 neat resin. This created laminates with fibers aligned in the direction of conductivity measurement or at a specified angle θ to it (see Fig. 1b).

As shown in Fig. 1, the x and y directions are defined as being in-plane for both the T^3 and IP measurements. The through-thickness z direction is defined as being out-of-plane in both cases.

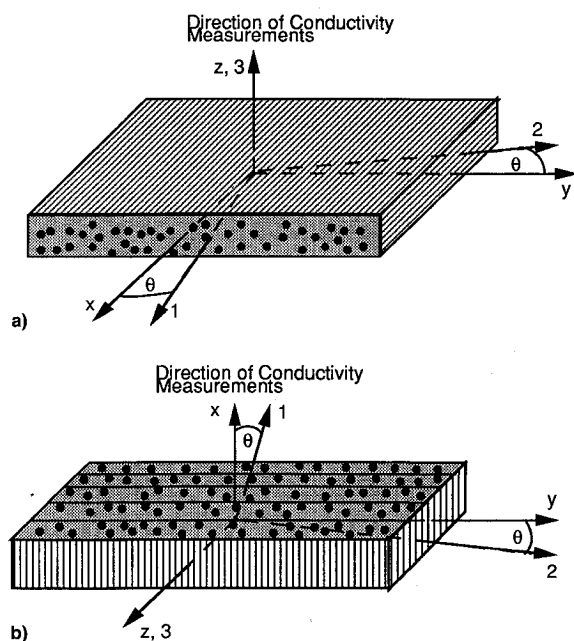
Slabs of 3501-6 neat resin were cured under vacuum in an oven at 177°C for up to 10 h. The slabs were 5.1 ± 0.25 mm thick, and were circular with a diameter of 12.7 ± 0.25 cm. The void content of the cured neat resin slabs was measured to be less than 2%, which did not change for various resin degrees of cure, $0.5 \leq \alpha \leq 0.98$.

Experimental Setup

A Dynatech TCFGM guarded hot plate, depicted in Fig. 2, was used to measure the thermal conductivity of the graphite/epoxy laminates and resin slabs. The thermal conductivity of the composite laminates was measured for the T^3 and IP laminates in the directions defined by Fig. 1. The guarded hot plate is designed for measuring the thermal performance of materials with a relatively low thermal conductivity. The material tested must also be opaque and should ideally be homogeneous and isotropic. These last two material requirements are not always met when testing an advanced composite; therefore, special precautions must be taken to minimize the experimental error. The experimental precautions taken to compensate for these two requirements will be discussed in this section.

The important components of the system included a guarded isothermal hot-surface plate (main heater) with an auxiliary isothermal cold-surface plate on either side. The main heater diameter was approximately 10.1 cm and that of the concentric guard heater, which maintains the same temperature as the main heater, was 20.2 cm. These heaters were separated by a gap of 1.52 mm. Cooling plates were used as heat sinks at both ends of the stack to prevent the stack from overheating. Composite laminates were placed between the isothermal surfaces, one on each side of the hot plate. The test method, therefore, simultaneously measured and averaged the properties of two nearly identical laminates. Each data point presented in this article is therefore the averaged property of two nearly identical composite laminates.

Establishment of idealized conditions within the guarded hot plate stack meant that there were no radial components of heat flux (this was experimentally verified); therefore, the thermal conductivity of the laminate in the direction normal to the isothermal plane was measured (see Direction of Conductivity Measurements in Fig. 1) under steady-state conditions. In general, 5–10 h were necessary for the stack to achieve equilibrium; the setup was not considered to be in equilibrium until the measured temperatures changed less than 0.1°C in a half hour.



T^3 and IP Measurements - Definition of Coordinate Systems:

Laminate Coordinate System	Ply Coordinate System
X Longitudinal	1 Longitudinal
Y Transverse	2 Transverse
Z Through-Thickness Transverse	3 Through-Thickness Transverse

Fig. 1 Definition of coordinate systems for the experimental thermal conductivity measurements. The one- and two-ply coordinates are rotated about the laminate z axis by the angle θ : a) T^3 and b) IP laminate measurements.

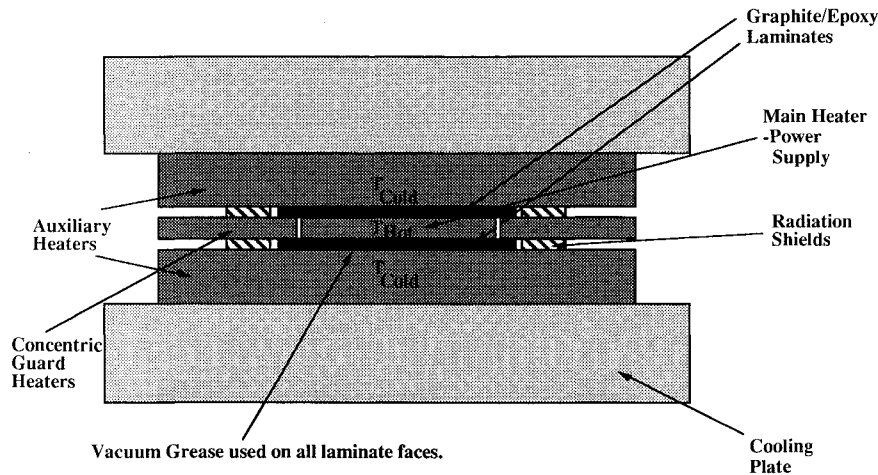


Fig. 2 Experimental setup enclosed in a vacuum for the thermal conductivity experiments using a guarded hot plate apparatus.

After all pieces of the stack were assembled, a compression plate was lowered onto it and 10–20 kg of force was applied using a spring mechanism. The entire stack was placed under a bell jar and a vacuum was applied. A Varian SD 300 vacuum pump was first used to remove the moisture (15–20 min), and then a Varian Turbo-V200 vacuum pump was used to achieve a vacuum on the order of 10^{-4} torr. The vacuum reduced convection away from the stack and across the gap between the main and guard heaters to a negligible level.

Limiting radiation of energy away from the stack was also important. The two critical areas where radiation was limited were 1) away from the main heater and 2) away from the composite laminates. The concentric guard heater balanced radiation from the main heater, and silicone insulation was placed around the edges of the composite laminates. Finally, a grease (G-9030 silicone high vacuum grease, McGhan Nusil Corp.) was applied in a thin layer to both faces of all tested laminates. In the vacuum, this grease was necessary to promote contact between the laminates and the aluminum plates, but it was also found to be a source of thermal resistance between the stack's plates and the composite laminates. This contact resistance was measured and accounted for as a resistance in series with the composite laminate. Using materials in series:

$$\frac{t_{\text{comp}} + t_c}{K_{\text{meas}}} = \frac{t_{\text{comp}}}{K_{\text{act}}} + \frac{t_c}{K_c} \quad (1)$$

The factor K_c/t_c was measured to be $7280 \pm 300 \text{ W/m}^2\text{°C}$ and will be referred to as the thermal contact conductance H_c of the experimental setup. The thermal contact conductance was measured over a range of temperatures (60–175°C) and contact forces. This temperature range is typical for cure cycles used to cure thermosetting composite materials. One value for H_c was proven to be statistically significant over this range of test temperatures and was used to calculate all actual thermal conductivities presented in this article as experimental data.

The experimental uncertainty for the thermal conductivity measurements was calculated to be $\pm 4.3\%$; the experimental uncertainty is represented in each of the article's figures by error bars, which are shown as $\pm 4.3\%$ of each data point presented. Six physical properties were measured to calculate each experimental thermal conductivity data point presented in this article. The voltage across the stack's heater and the current flowing to the heater were measured; the error in these measurements was considered to be insignificant. The area of the main heater plate was estimated to be known within $\pm 0.6\%$, and the thickness of each composite laminate within $\pm 1\%$. The uncertainty of the measured temperature difference across the stack was estimated to be $\pm 1.2\%$. Finally, the contact conductance between the laminates and the stack was mea-

sured over a range of temperatures, 60–175°C, and contact forces; the uncertainty of the contact conductance was measured to be $\pm 4.1\%$. The total experimental uncertainty was calculated, based upon the six individual experimental uncertainties, to be $\pm 4.3\%$. A more detailed discussion on the experimental uncertainty for this research can be found elsewhere.⁷

Through-Thickness Transverse Thermal Conductivity

Through-Thickness Transverse Conductivity vs the Resin Degree of Cure

The effect resin energy generation has on the measured thermal conductivity of an uncured or partially cured thermosetting composite is of interest for experiments conducted when the resin is not fully cured. The idea is to determine the thermal conductivity of a laminate with ongoing endothermic or exothermic reactions when the resin energy generation rate is known from neat resin cure kinetics equations.

In a previous paper⁸ it was shown that the resin energy generation term is given by

$$\dot{q} = \rho_{\text{comp}} \frac{d\alpha}{dt} H_r \quad (2)$$

where H_r was measured to be $156 \pm 4 \text{ J/g}$ for AS4/3501-6, and $d\alpha/dt$ is the reaction rate of the resin. It was also shown that the effective thermal conductivity of a thermosetting composite with ongoing resin chemical reactions is

$$K_{\text{eff}} = \frac{dx}{dT} \left(q_{\text{in}} + \frac{\dot{q}^* t}{2} \right) \quad (3)$$

Other researchers⁹ have measured that the thermal conductivity of a thermosetting composite may vary significantly with changing resin degree of cure; however, these researchers did not account for the resin energy generation term. In this work, each laminate was first cured to a known resin degree of cure using the methods previously described. The laminate's degree of cure was verified using a differential scanning calorimeter (DSC)¹⁰ before its thermal conductivity was measured using the guarded hot plate. Small samples were then taken from each laminate before they were tested in the guarded hot plate. After curing of each laminate occurred during the actual thermal conductivity measurement, its sample was put through the same temperature cycle as that for the guarded hot plate experiment. The resin energy generation and degree of cure for each sample was measured again using the DSC. This was

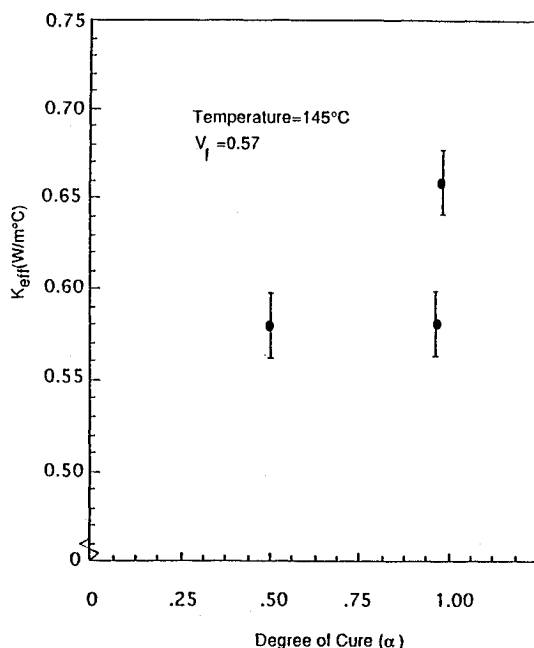


Fig. 3 Through-thickness transverse thermal conductivity experimental data of unidirectional AS4/3501-6 graphite/epoxy laminates cured to various degrees of cure.

used as the resin degree of cure for each thermal conductivity measurement.

Figure 3 shows the experimentally measured through-thickness transverse thermal conductivity of the T³ laminates cured to various resin degrees of cure. Notice that when the resin energy generation is accounted for within the laminate, the effective conductivity is constant with increasing resin degree of cure through $\alpha = 0.96$. There, however, is a 13% increase in the laminate thermal conductivity at $\alpha = 0.98$.

The thermal conductivity of 3501-6 neat resin slabs, cured to various degrees of cure, was measured. It was found that a small increase in conductivity ($\approx 2\%$ occurs for $0.80 \leq \alpha \leq 0.96$ and another 2% for $0.96 \leq \alpha \leq 0.98$). The resin density was also measured to increase 3.1% from 1.26 to 1.30 g/cm³, with no measured change in void content, for $0.96 \leq \alpha \leq 0.98$. It is therefore likely that the increase in thermal conductivity of a laminate for $0.96 \leq \alpha \leq 0.98$ is because of a small increase in resin conductivity, as well as an increase because of resin shrinkage upon final cure, which effectively increases the fiber volume fraction of the laminate, and its through-thickness transverse thermal conductivity.

Through-Thickness Transverse Conductivity vs the Ply Lay-Up Angle

Previous researchers^{11,12} have stated that the thermal conductivity of an advanced composite is a transversely isotropic property of the material. This suggests that the through-thickness transverse thermal conductivity of a laminate should not vary with its constituent ply's lay-up angles. That is, a unidirectional laminate should have the same through-thickness transverse conductivity as a laminate with multiangled plies. Others,¹³ however, have found that the through-thickness transverse thermal conductivity of multiangled laminates is less than that of unidirectional laminates of the same fiber volume fraction.

In a previous paper,⁸ the transversely anisotropic behavior of multiangled laminates was modeled using a variation of Rayleigh's¹⁴ model for cylinders arranged in rectangular order. When the statistically averaged resin rectangle around a typical fiber within a laminate has a moderate aspect ratio (width/

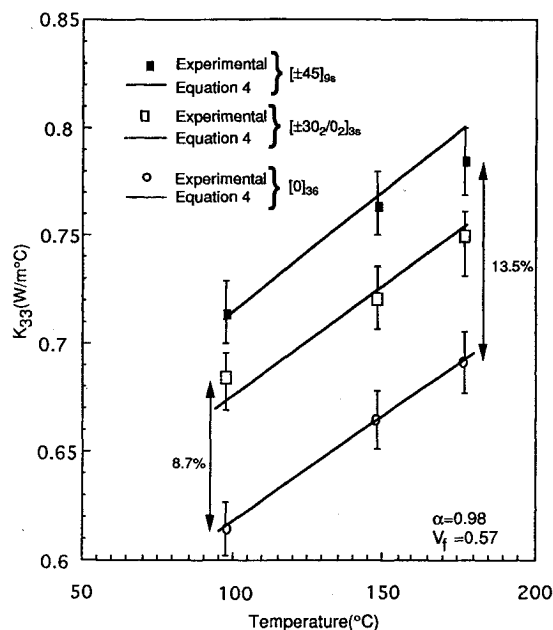


Fig. 4 Equation (4) vs the through-thickness transverse thermal conductivity experimental data.

height not much greater than 1.0), the approximate through-thickness conductivity K_{33} for a laminate may be calculated

$$\frac{K_{33}}{K_r} \cong 1 - \frac{2p}{\nu' + p - (3p^4/\nu'\pi^4)S_4^2 - (7p^8/\nu'\pi^8)S_8^2 \dots} \quad (4)$$

where

$$\nu' = [(K_r/K_f) + 1]/[(K_r/K_f) - 1] \quad (5)$$

$$p = V_f(\epsilon/\delta) \quad (6)$$

Here, δ is the dimension of the average resin rectangle around a typical fiber parallel to the direction of conductivity measurement (height) and ϵ the dimension perpendicular to the measurement direction (width):

$$S_4 = 3.151 \quad S_8 = 4.256 \quad (7)$$

Figure 4 shows the experimentally measured through-thickness transverse conductivity of T³ laminates with various ply lay-up angles. It is seen that the through-thickness transverse thermal conductivity of a $(\pm 30^\circ/0^\circ)_{3s}$ laminate is approximately 8.7% greater than that of a unidirectional laminate $[0]_{3s}$, and that the $[\pm 45]_{9s}$ laminate has a measured conductivity of about 13.5% greater than the unidirectional case. At the same fiber volume fraction and temperature, an explanation for this phenomenon is that the fibers of the multiangled laminates have settled closer together during cure (in the measured through-thickness direction) than the fibers of a unidirectional laminate. This was found to be the case using photomicrographs of the laminate's cross sections. The average resin rectangle around a fiber in the unidirectional case was measured to have a side aspect ratio of $\epsilon/\delta = 1.02$. The ratio for the $[\pm 30^\circ/0^\circ]_{3s}$ laminate was measured to be $\epsilon/\delta = 1.06$ and the ratio of the $[\pm 45]_{9s}$ laminate was $\epsilon/\delta = 1.10$.

The analytical model of Eq. (4) is plotted with the experimental data in Fig. 4. Figure 4 shows that, based on the typical resin element aspect ratio, the model predicts the increase in conductivity for multiangled laminates as compared to a unidirectional laminate very well. This model is valid only for aspect ratios near $\epsilon/\delta = 1.0$, and has not been experimentally validated for aspect ratios greater than $\epsilon/\delta = 1.10$.

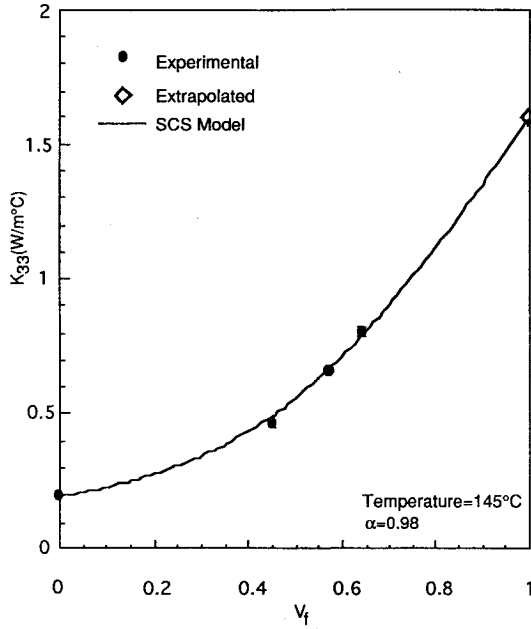


Fig. 5 Equation (10) (SCS model) plotted vs the through-thickness transverse thermal conductivity experimental data of unidirectional laminates.

Through-Thickness Transverse Conductivity vs the Fiber Volume Fraction

The through-thickness transverse thermal conductivity of a unidirectional composite material is also a function of its fiber volume fraction (the fibers have a higher conductivity than the resin). Many models¹⁴⁻¹⁹ have been proposed to describe this property, but most make assumptions about fiber packing geometry that preclude their use when this geometry is unknown or random. A model using a self-consistent scheme (SCS) has been derived for the effective through-thickness thermal conductivity of a laminate with fibers packed in resin.⁷ The derivation of this model is similar to that derived for spherical particulates²⁰ in a resin matrix. The model is said to account for fiber-fiber interaction, the percolation effect,²¹⁻²³ and makes no assumptions about fiber packing geometry.

The fundamental assumption of the SCS method is that a typical element of the heterogeneous materials can be thought of as being embedded in an effective homogeneous material that has volume-averaged properties of the two constituent materials. The effective property (i.e., the averaged macroscopic conductivity) is calculated using a far-field boundary condition, boundary conditions at the typical element/effective material boundary, and field equations defined for each region.

When the only laminate information known are the fiber and resin volume fractions and that the laminate has unidirectional fibers, an upper and lower bound can be derived, as well as a family of intermediate curves for the through-thickness transverse conductivity of the laminate. The best possible lower bound is

$$\frac{K_{33}^L}{K_r} = \frac{[1 + (K_f/K_r)] + V_f[(K_f/K_r) - 1]}{[1 + (K_f/K_r)] - V_f[(K_f/K_r) - 1]} \quad (8)$$

and the best possible upper bound is

$$\frac{K_{33}^U}{K_f} = \frac{[1 + (K_r/K_f)] + V_r[(K_r/K_f) - 1]}{[1 + (K_r/K_f)] - V_r[(K_r/K_f) - 1]} \quad (9)$$

The intermediate equation chosen for this article is

$$\frac{K_{33}}{K_r} = \frac{1}{2} \left\{ V_f \gamma + (1 - \nu) + \gamma \left[V_f^2 - V_f + \frac{(\nu + 1)^2}{\gamma^2} \right]^{1/2} \right\} \quad (10)$$

where γ is defined as

$$\gamma = (2\nu - 2) \quad (11)$$

and $\nu = K_f/K_r$.

Once again, the bounds have been shown to be the best possible when only the material conductivities and their respective volume fractions have been specified.²⁰ Equation (10) represents a model where the typical fiber was considered to be directly embedded in the effective material, and it predicts values that are always between the two prescribed boundaries.

Figure 5 shows the experimentally measured through-thickness transverse thermal conductivity of unidirectional T³ laminates plotted vs the model of Eq. (10). Figure 5 shows that the model predicts the experimental data within the experimental uncertainty of the test at 145°C. Experimental tests were also conducted at 95 and 175°C with similar results,⁷ but are not shown here. It is also seen that the model predicts a graphite fiber transverse thermal conductivity of 1.60 W/m°C at 145°C. The fiber thermal conductivity is an extrapolation of the experimental data using the SCS model to generate a best-curve fit of the other four data points. Similar measurements and extrapolations at 95 and 175°C predict a graphite fiber transverse thermal conductivity of 1.55 and 1.65 W/m°C, respectively.

In-Plane Thermal Conductivity

Longitudinal Thermal Conductivity vs the Fiber Volume Fraction

In the ply longitudinal direction (the 1 direction of Fig. 1) the continuous graphite fibers are idealized to be in parallel combination with the resin for a unidirectional laminate. Because of this, a simple rule of mixtures is used to describe the longitudinal thermal conductivity K_{11} of the laminate:

$$K_{11} = K_f V_f + K_r V_r \quad (12)$$

Figure 6 shows the experimentally measured longitudinal thermal conductivities of unidirectional IP laminates plotted vs the Eq. (12) model. It is seen that the model represents the experimental data very well and that the extrapolated longitudinal thermal conductivity of the AS4 graphite fibers is 11.3 W/m°C at 145°C. Similar measurements and extrapolations at 95 and

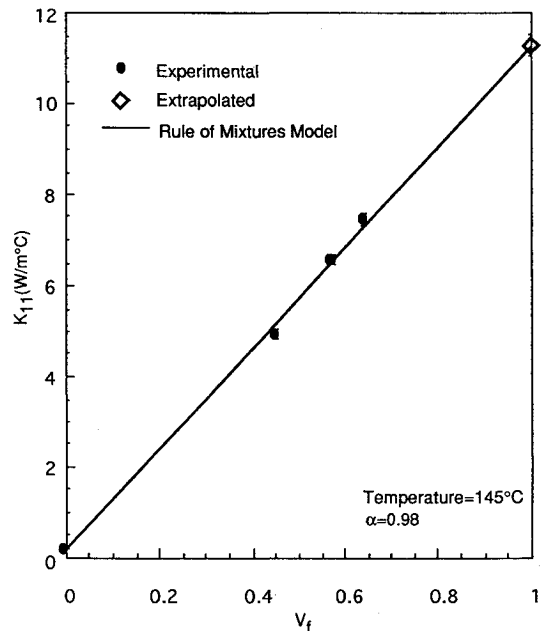


Fig. 6 Equation (12) vs the in-plane longitudinal thermal conductivity experimental data of unidirectional laminates.

175°C predict a graphite fiber longitudinal thermal conductivity of 10.0 and 11.9 W/m°C, respectively.⁷

In-Plane Thermal Conductivity with Plies Rotated at One Angle

Once the laminate principal conductivities (K_{33} and K_{11}) have been measured, it is necessary to have a method enabling the in-plane rotation of these principal conductivities into another axis system. A second-order tensor transformation of the principal conductivities has generally been suggested for this purpose.^{11,24} Bogetti and Gillespie²⁵ used the mathematics of this transformation in their two-dimensional heat transfer model. However, this transformation has not been experimentally validated for a fiber-reinforced composite. Grove et al.²⁶ describe an experimental setup using a guarded hot plate with a long rod configuration, detail the manufacture of their specimens, but do not present their experimental results.

Harris et al.²⁷ and Pilling et al.²⁸ used a version of the guarded hot plate to experimentally study this transformation rule. The difference between their experimental and theoretical results is clearly greater than the experimental error for their tests. A possible reason for their discrepancies is the contact conductance (as previously described) between the composite specimen and their test apparatus. Havis et al.²⁹ also study the transformation rule, but their experimental data do not always match the mathematics of the transformation, even within a 90% confidence range. These researchers experienced edge effect difficulties in their experiments. A paper published by Hasselman et al.³⁰ demonstrates that the test specimen's geometry greatly effects the in-plane thermal conductivity experimental results for a laminate with plies rotated away from the direction of conductivity measurement.

As described earlier, an experimental setup was designed to minimize laminate edge-effects during the thermal measurements, as well as to account for any effect that specimen geometry or specimen contact conductance might have on the measurements. The experimental setup included silicone insulation surrounding the laminates, and the IP laminate measurements were taken using relatively thin laminates (5.1 mm thick), to minimize energy loss at the laminates' edges. The contact resistance H_c between the laminates and the experimental setup was also measured.

Accounting for the contact resistance is important when measuring the lower thermal conductivities transverse to the fibers because discrepancies of 3–4% were found between actual and measured conductivities. It becomes absolutely necessary when measuring the higher thermal conductivities parallel to the direction of the fibers, where discrepancies of 25–30% were found between actual and measured conductivities. Accounting for contact resistance is also necessary when comparing through-thickness transverse and longitudinal principal conductivities to measurements of laminates with plies rotated between these two principal directions.

A second-order tensor transformation is used to rotate the principal thermal conductivities into another in-plane axes system.¹⁰ The conductivity measured in the x direction (see Fig. 1b) is defined as

$$K_{xx}^{\theta} = K_{11} \cos^2 \theta + K_{33} \sin^2 \theta \quad (13)$$

Figure 7 shows the experimentally measured conductivity values for IP laminates with plies rotated 30 and 45 deg in-plane to the direction of conductivity measurement compared to the analytical values calculated using Eq. (13). Values from Fig. 5 ($V_f = 0.57$) were used for K_{33} , and values from Fig. 6 ($V_f = 0.57$) were used for K_{11} in the calculations of Eq. (13). Figure 7 shows that Eq. (13) predicts the experimental measurements of K_{xx} within the experimental uncertainty throughout the temperature range of 95–175°C.

In Figure 8, the experimental results are also plotted vs the angle of ply rotation θ and compared to Eq. (13) at 145°C using IP laminates with a $V_f = 0.57$. In this figure, the 0-deg

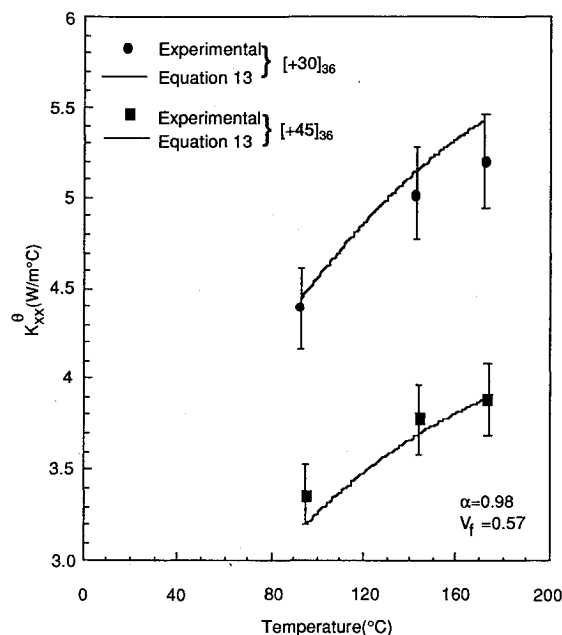


Fig. 7 Equation (13) vs the in-plane thermal conductivity experimental data of unidirectional laminates with plies rotated away from the direction of conductivity measurement.

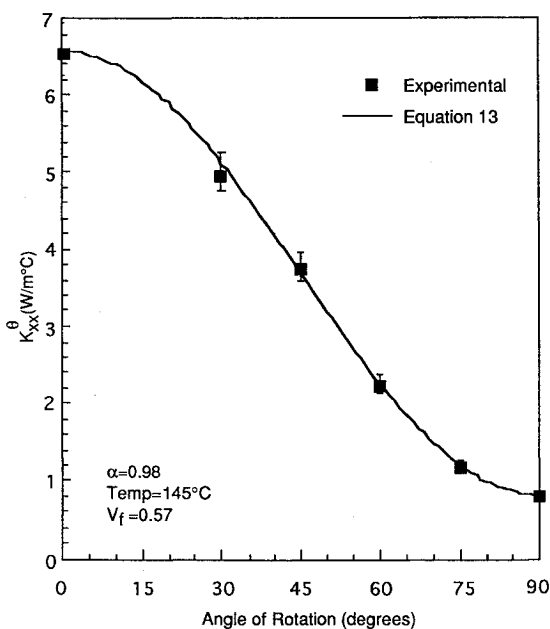


Fig. 8 Equation (13) vs the in-plane thermal conductivity experimental data of unidirectional laminates with rotated plies at angles from 0 to 90 deg.

data point is the experimentally measured longitudinal conductivity of Fig. 6, and the 90-deg data point is that of the experimentally measured through-thickness transverse conductivity of Fig. 5. The other data points were measured using IP laminates with in-plane rotation angles of 30, 45, 60, and 75 deg to the direction of conductivity measurement. These results validate the experimental setup and it is concluded that the second-order tensor rotation has been experimentally verified for the thermal conductivity of these laminates.

Laminates with $\pm\theta$ combinations of plies were also experimentally measured. The second-order tensor transformation of Eq. (13) predicts that the conductivity of a laminate composed of $\pm\theta$ plies will be the same as one composed of $\pm\theta$ plies. However, Fig. 9 shows that the conductivity of the $+\theta$ IP laminate is generally a few percent higher than that of the

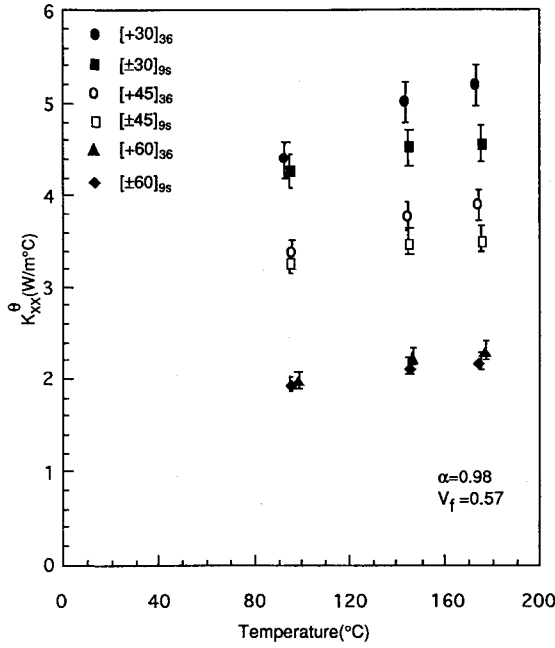


Fig. 9 Comparison of the in-plane thermal conductivity experimental data for laminates with $+\theta$ and $\pm\theta$ plies.

corresponding $\pm\theta$ IP laminate. It has not been determined if this discrepancy is of a theoretical or experimental nature.

In-Plane Thermal Conductivity with Plies Rotated at Multiple Angles

A parallel-combination of the individual-ply second-order tensor transformations can be used when the in-plane conductivity of laminates with various ply angles of rotation is measured. The macrothermal behavior of the laminate is desired in steady state, and the classical laminated plate theory (CLPT), which is used to model the macromechanical behavior of laminates, provides an analogous derivation. The macromechanical behavior of a laminate using the CLPT is given by Jones.³¹ Ghasemi Nejhad et al.⁶ have also used this approach to model the thermal properties of thermoplastic matrix composites.

For the given problem, the heat flux per unit area is in the x and y directions (q_x, q_y), with x being in the direction of conductivity measurement and y being perpendicular to it (see Fig. 1b). As used throughout this article, the x and y directions are defined as being in-plane, and the z direction is defined as being out-of-plane. An applied temperature gradient exists only in the x direction. The total heat flux is given by

$$\begin{aligned} Q_x &= W \int_{-t/2}^{t/2} q_x \, dz \\ Q_y &= L \int_{-t/2}^{t/2} q_y \, dz \end{aligned} \quad (14)$$

For a laminated plate, Eq. (14) becomes the sum of the integrals across each of the plies

$$\begin{aligned} Q_x &= W \sum_{k=1}^N \int_{z_{k-1}}^{z_k} q_x \, dz \\ Q_y &= L \sum_{k=1}^N \int_{z_{k-1}}^{z_k} q_y \, dz \end{aligned} \quad (15)$$

where z_k is the top and z_{k-1} is the bottom of each individual

ply as one moves away from the laminate centerline ($z = 0$). With an applied temperature gradient $T_{,x}$ in the x direction only

$$\begin{aligned} q_x &= -K_{xx}^\theta T_{,x} \\ q_y &= -K_{xy}^\theta T_{,x} \end{aligned} \quad (16)$$

Then

$$\begin{aligned} Q_x &= -W \sum_{k=1}^N K_{xx}^\theta \int_{z_{k-1}}^{z_k} T_{,x} \, dz \\ Q_y &= -L \sum_{k=1}^N K_{xy}^\theta \int_{z_{k-1}}^{z_k} T_{,x} \, dz \end{aligned} \quad (17)$$

and because $T_{,x}$ does not vary in the z direction:

$$\begin{aligned} Q_x &= -W^* T_{,x} \left[\sum_{k=1}^N K_{xx}^\theta (z_k - z_{k-1}) \right] \\ Q_y &= -L^* T_{,x} \left[\sum_{k=1}^N K_{xy}^\theta (z_k - z_{k-1}) \right] \end{aligned} \quad (18)$$

Normalizing with respect to specimen thickness t , we can define the bracketed expressions as

$$\begin{aligned} K_{xx} &= \frac{1}{t} \sum_{k=1}^N K_{xx}^\theta t_k \\ K_{xy} &= \frac{1}{t} \sum_{k=1}^N K_{xy}^\theta t_k \end{aligned} \quad (19)$$

where $t_k = (z_k - z_{k-1})$ is the thickness of each ply within the laminate and t is the total thickness of the laminate in the z direction. As calculated using Eq. (19), K_{xx} is the in-plane conductivity measured in the x direction (see Fig. 1b) and Eq. (13) is used to calculate each ply's conductivity K_{xx}^θ .

Figure 10 shows the experimental results plotted vs the calculated values for a $[\pm 30_2/O_2]_{3s}$ and a $[\pm 60_2/O_2]_{3s}$ laminate. For the $[\pm 30_2/O_2]_{3s}$ laminate, a combination of ± 30 deg (Fig.

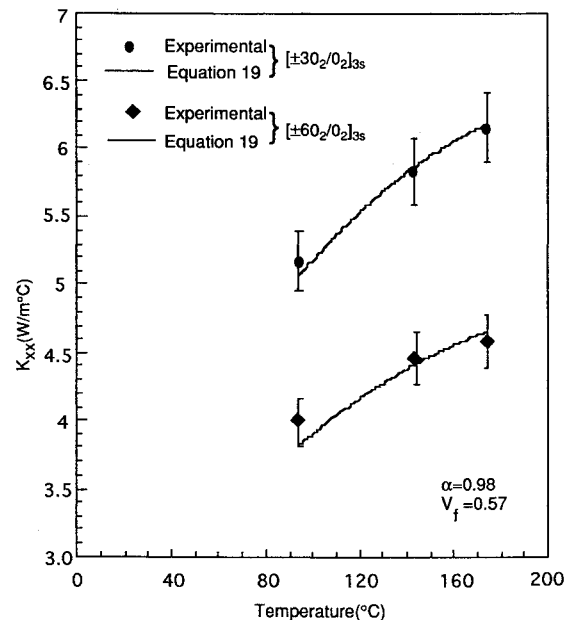


Fig. 10 Equation (19) vs the in-plane thermal conductivity experimental data of laminates with various different angles of rotation.

Table 1 Extrapolated values for the transverse and longitudinal thermal conductivity of AS4 fibers as well as the measured thermal conductivity of 3501-6 neat resin ($\alpha = 0.98$)

K, W/m°C	95°C	145°C	175°C
AS4 fiber-longitudinal	10.0	11.3	11.9
AS4 fiber-transverse	1.55	1.60	1.65
3501-6 resin	0.255	0.270	0.283

9) and 0 deg (Fig. 6) longitudinal plies were used to calculate the analytical K_{xx} values of Eq. (19). Similar calculations were completed for the $[\pm 60_2/O_{213}]_s$ laminate. The analytical model of Eq. (19) is seen to predict the experimental values within the experimental uncertainty throughout the temperature range of 95–175°C.

Constituent Materials' Thermal Conductivity

Table 1 shows the experimentally measured thermal conductivity of fully cured ($\alpha = 0.98$) 3501-6 neat resin. The analytically extrapolated values for the transverse thermal conductivity of AS4 fibers [based on the SCS method, Eq. (10), Fig. 5], and the longitudinal thermal conductivity of AS4 fibers [based on the rule of mixtures method, Eq. (12), Fig. 6] are also shown. The analytically extrapolated thermal conductivity values for the AS4 fibers are important because it is very difficult to directly measure the thermal conductivity of the graphite fibers.

Conclusions

The thermal conductivity of a thermosetting advanced composite material during its cure was experimentally investigated and compared to analytical models. Techniques for manufacturing composite laminates with various resin degrees of cure, as well as through-thickness transverse and in-plane properties such as fiber volume fraction and different ply lay-up angles, were described. A guarded hot plate experimental apparatus and setup necessary for accurate through-thickness transverse and in-plane thermal conductivity measurements were also described.

The through-thickness transverse thermal conductivity of composite laminates was experimentally measured at various resin degrees of cure and fiber volume fractions while using different ply lay-up angles. Equations that include the resin energy generation within the composite, enabling the calculation of the laminate thermal conductivity during resin cure, were presented. Equations that account for variances in fiber proximity were presented and a self-consistent scheme was used to accurately model the composite through-thickness transverse thermal conductivity of a laminate vs its fiber volume fraction.

The in-plane thermal conductivity was measured using unidirectional laminates, as well as laminates with various ply lay-up angles. A rule of mixtures equation that models the longitudinal thermal conductivity with respect to the laminate fiber volume fraction, as well as a second-order tensor transformation that rotates the principal conductivities into another in-plane axes system, were presented. Techniques from the classical laminated plate theory were adapted to derive equations that describe the in-plane thermal conductivity of laminates with plies rotated at multiple angles. All of these analytical models were shown to represent the measured data within the calculated experimental uncertainty.

Acknowledgments

This research was funded through the Leaders for Manufacturing program at the Massachusetts Institute of Technology, with Richard McLane of The Boeing Company acting as the Technical Sponsor. The authors wish to acknowledge the generous support of Charles Haldeman and Ron Efromson of the

Massachusetts Institute of Technology Lincoln Laboratory, who donated the guarded hot plate equipment for the thermal conductivity experiments and provided valuable technical support throughout this research.

References

- Loos, A. C., and Springer, G. S., "Curing of Epoxy Matrix Composites," *Journal of Composite Materials*, Vol. 17, 1983, pp. 135–169.
- Scott, E. P., and Beck, J. V., "Estimation of Thermal Properties in Carbon/Epoxy Composite Materials During Cure," *Journal of Composite Materials*, Vol. 26, No. 1, 1992, pp. 20–36.
- Mijovic, J., and Wijaya, J., "Effects of Graphite Fiber and Epoxy Matrix Physical Properties on the Temperature Profile Inside Their Composite During Cure," *SAMPE Journal*, Vol. 25, No. 2, 1989, pp. 35–39.
- Gutowski, T. G., Morigaki, T., and Cai, Z., "The Consolidation of Laminate Composites," *Journal of Composite Materials*, Vol. 21, 1987, pp. 172–188.
- Cai, Z., "Simulation of the Manufacture of Closed Shape Composite Structures," Ph.D. Dissertation, Massachusetts Inst. of Technology, Cambridge, MA, 1990.
- Ghasemi Nejhad, M. N., Cope, R. D., and Güçeri, S. I., "Thermal Analysis of In-Situ Thermoplastic-Matrix Composite Filament Winding," *Journal of Heat Transfer*, Vol. 113, No. 2, 1991, pp. 304–313.
- Farmer, J. D., "Heat Transfer in an Anisotropic Thermosetting Advanced Composite During Its Cure," M.S. Thesis, Massachusetts Inst. of Technology, Cambridge, MA, 1993.
- Farmer, J. D., and Covert, E. E., "Transverse Thermal Conductance of Thermosetting Composite Materials During Their Cure," *Journal of Thermophysics and Heat Transfer*, Vol. 8, No. 2, 1993, pp. 358–365.
- Mijovic, J., and Wang, H. T., "Modeling of Processing of Composites Part II—Temperature Distribution During Cure," *SAMPE Journal*, Vol. 22, 1988, pp. 42–55.
- Lee, W. I., Loos, A. C., and Springer, G. S., "Heat of Reaction, Degree of Cure and Viscosity of Hercules 3501-6 Resin," *Journal of Composite Materials*, Vol. 16, No. 11, 1982, pp. 510–520.
- Tsai, S. W., and Hahn, H. T., *Introduction to Composite Materials*, Technomic Publishing Co., Inc., New York, 1980, pp. 329–333.
- Humphreys, E. A., and Rosen, B. W., "Properties Analysis of Laminates," *Engineered Materials Handbook: Composites*, edited by T. J. Reinhart, Vol. 1, ASM International, New York, 1992, pp. 218–235.
- Scott, E. P., and Beck, J. V., "Estimation of Thermal Properties in Epoxy Matrix/Carbon Fiber Composite Materials," *Journal of Composite Materials*, Vol. 26, 1992, pp. 132–149.
- Rayleigh, L., "On the Influence of Obstacles Arranged in Rectangular Order upon the Properties of a Medium," *Philosophical Magazine*, Vol. 34, 1892, pp. 481–503.
- Springer, G. S., and Tsai, S. W., "Thermal Conductivities of Unidirectional Materials," *Journal of Composite Materials*, Vol. 1, 1967, pp. 166–173.
- Behrens, E., "Thermal Conductivities of Composite Materials," *Journal of Composite Materials*, Vol. 2, 1968, pp. 2–17.
- Thornborough, J. D., and Pears, C. D., American Society of Mechanical Engineers, Paper 65-WA/HT 4, March 1965.
- Han, L. S., and Cosner, A. A., "Effective Thermal Conductivities of Fibrous Composites," *Journal of Heat Transfer*, Vol. 103, 1981, pp. 387–392.
- Hashin, Z., and Shtrikman, S., "A Variational Approach to the Theory of the Effective Magnetic Permeability of Multiphase Materials," *Journal of Applied Physics*, Vol. 33, 1962, pp. 3125–3131.
- Hashin, Z., "Assessment of the Self Consistent Scheme Approximation: Conductivity of Particulate Composites," *Journal of Composite Materials*, Vol. 2, 1968, pp. 284–300.
- Polder, D., and Van Santen, J. H., "The Effective Permeability of Mixtures of Solids," *Physica XII*, Vol. 5, 1946, pp. 257–271.
- Bergman, D. J., "Analytical Properties of the Complex Effective Dielectric Constant of a Composite Medium with Applications to the Derivation of Rigorous Bounds and to Percolation Problems," *Electrical Transport and Optical Properties of Inhomogeneous Media*, edited by J. C. Garland and D. B. Tanner, American Inst. of Physics, New York, 1978, pp. 46–62.
- Kirkpatrick, S., "The Geometry of the Percolation Threshold," *Electrical Transport and Optical Properties of Inhomogeneous Media*, edited by J. C. Garland and D. B. Tanner, American Inst. of Physics,

New York, 1978, pp. 99–116.

²⁴Ozisik, M. N., *Boundary Value Problems of Heat Conduction*, International Textbook, London, 1968, pp. 455–477.

²⁵Bogetti, T. A., and Gillespie, J. W., Jr., "Two-Dimensional Cure Simulation of Thick Thermosetting Composites," *Journal of Composite Materials*, Vol. 25, 1991, pp. 239–273.

²⁶Grove, S. M., Short, D., and Bacon, D. H., "Anisotropic Heat Conduction in Fibre Composites," *13th Reinforced Plastics Conference* (Brighton, England, UK), 1982, pp. 249–252.

²⁷Harris, J. P., Yates, B., Batchelor, J., and Garrington, P. J., "The Thermal Conductivity of Kevlar Fibre-Reinforced Composites," *Journal of Materials Science*, Vol. 17, 1982, pp. 2925–2931.

²⁸Pilling, M. W., Yates, B., Black, M. A., and Tattersall, P., "The

Thermal Conductivity of Carbon Fibre-Reinforced Composites," *Journal of Materials Science*, Vol. 14, 1979, pp. 1326–1338.

²⁹Havis, C. R., Peterson, G. P., and Fletcher, L. S., "Predicting the Thermal Conductivity and Temperature Distribution in Aligned Fiber Composites," *Journal of Thermophysics and Heat Transfer*, Vol. 3, 1990, pp. 416–422.

³⁰Hasselman, D. P. H., Bhatt, H., Donaldson, K. Y., and Thomas, J. R., "Effect of Fiber Orientation and Sample Geometry on the Effective Thermal Conductivity of a Uniaxial Carbon Fiber-Reinforced Glass Matrix Composite," *Journal of Composite Materials*, Vol. 26, 1992, pp. 2278–2288.

³¹Jones, R. M., *Mechanics of Composite Materials*, Hemisphere, New York, 1975, pp. 147–172.

LIQUID ROCKET ENGINE COMBUSTION INSTABILITY

Vigor Yang and William E. Anderson, editors,
Propulsion Engineering Research Center,
Pennsylvania State University, University Park, PA

Since the invention of the V-2 rocket during World War II, combustion instabilities have been recognized as one of the most difficult problems in the development of liquid propellant rocket engines. This book is the first published in the U.S. on the subject since NASA's Liquid Rocket Combustion Instability (NASA SP-194) in 1972. Improved computational and experimental techniques, coupled with a number of experiences with full-scale engines worldwide, have offered opportunities for advancement of the state of the art. Experts cover four major subjects areas: engine

phenomenology and case studies, fundamental mechanisms of combustion instability, combustion instability analysis, and engine and component testing. Especially noteworthy is the inclusion of technical information from Russia and China, a first. Engineers and scientists in propulsion, power generation, and combustion instability will find the 20 chapters valuable as an extension of prior work and as a reference.

Contents (partial):

I. Instability Phenomenology and Case Studies

II. Fundamental Mechanisms of Combustion Instabilities

III. Combustion Instability Analysis

IV. Stability Testing Methodology

1995, 500 pp, illus, Hardback

ISBN 1-56347-183-3

AIAA Members \$64.95

List Price \$79.95

Order V-169(945)



American Institute of Aeronautics and Astronautics

Publications Customer Service, 9 Jay Gould Ct., P.O. Box 753, Waldorf, MD 20604
Fax 301/843-0159 Phone 1-800/682-2422 8 a.m. – 5 p.m. Eastern

Sales Tax: CA and DC residents add applicable sales tax. For shipping and handling add \$4.75 for 1–4 books (call for rates for higher quantities). Orders under \$100.00 must be prepaid. Foreign orders must be prepaid and include a \$20.00 postal surcharge. Please allow 4 weeks for delivery. Prices are subject to change without notice. Returns will be accepted within 30 days. Non-U.S. residents are responsible for payment of any taxes required by their government.